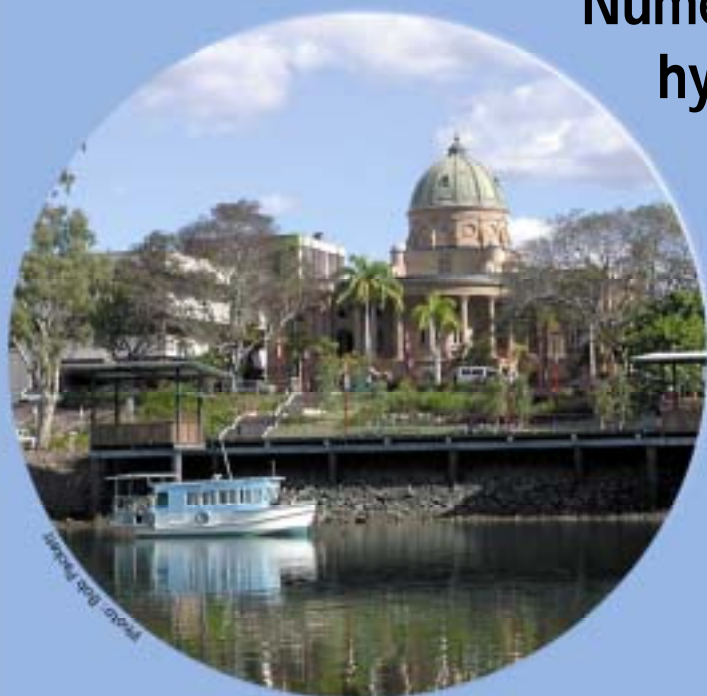




Cooperative Research Centre for Coastal Zone Estuary and Waterway Management

Technical Report 9



Numerical modelling of hydrodynamics, sediment transport and biogeochemistry in the Fitzroy Estuary

N. Margvelashvili, B. Robson, P. Sakov,
I.T. Webster, J. Parslow, M. Herzfeld,
J. Andrewartha

October 2003



CRC for Coastal Zone
Estuary & Waterway Management



**NUMERICAL MODELLING OF HYDRODYNAMICS,
SEDIMENT TRANSPORT AND BIOGEOCHEMISTRY IN
THE FITZROY ESTUARY**

Coastal CRC Final Report (Draft)

*N. Margvelashvili, B. Robson, P. Sakov, I.T. Webster, J. Parslow,
M. Herzfeld, J. Andrewartha*

CSIRO Marine Research
GPO Box 1538, Hobart 7001

CSIRO Land and Water
GPO Box 1666, Canberra 2601

October 2003

Acknowledgements

Ian Webster was responsible for planning and oversight of this project and editing of the final report. Development of the hydrodynamic model was conducted by Pavel Sakov, John Parslow, Mike Herzfeld and John Andrewartha. Pavel Sakov applied the hydrodynamic model to Fitzroy Estuary. Pavel Sakov and Nugzar Margvelashvili wrote the sections of the final report relating to hydrodynamic modelling. Development and application of the sediment model was by Nugzar Margvelashvili, who also wrote the associated sections of this report. Development of the biogeochemical model was by John Parslow, Pavel Sakov and Barbara Robson. Barbara Robson applied the biogeochemical model to Fitzroy Estuary and wrote the relevant sections of this report.

Preliminary tidal modelling of the estuary was conducted by Alan Griffiths and Pei Tillman. Barbara Robson was responsible for writing the Executive Summary and compiling this report.

Field data used in all phases of the model were collected during the Coastal CRC project Carbon and Nitrogen Cycling in a Subtropical Estuary (Ford et al. 2003). The biogeochemical model described here also relied on results from the nitrogen budgets calculated by Ian Webster and described in Ford et al. (2003).

Table of Contents

ACKNOWLEDGEMENTS	I
TABLE OF CONTENTS	II
EXECUTIVE SUMMARY	III
Background	iii
Results	iii
Outcomes and Further Work	iv
1 INTRODUCTION	1
2 MODEL DESCRIPTION AND SET UP	3
2.1 Model overview	3
2.1.1 Hydrodynamic and sediment models	3
2.1.2 Biogeochemical model	5
2.2 Numerical grid	7
2.3 Initial data and forcing	8
2.3.1 Point sources	13
3 MODEL SIMULATIONS	13
3.1 Hydrodynamics	14
3.2 Sediments	17
3.2.1 Sediment model vs observations	17
3.2.2 Sediment redistribution and fluxes	22
3.3 Biogeochemistry	29
4 CONCLUSIONS	34
5 REFERENCES	37
APPENDIX 1. PARAMETER VALUES USED IN THE SEDIMENT AND BIOGEOCHEMICAL MODEL.	39

Executive summary

Background

The Fitzroy is a very large catchment with an extensive wetland delta and estuarine area that is a major fisheries habitat for central Queensland. Significant loads of sediments and nutrients from the catchment are transported through the estuary. Within the estuary, sediments and nutrients are subject to physical and biological processes that can alter their form or remove them from the water column. The impacts of varying flows and contaminant loads on the health and ecology of the estuary are largely unknown, and the role of the estuary in processing contaminants from the catchment before they reach Keppel Bay has not yet been quantified.

This report describes the development of numerical models for the estuary as a first step towards quantifying these impacts and linkages. The project has three key components, specifically: 1. hydrodynamic modelling; 2. sediment and turbidity modelling; and 3. modelling of biogeochemistry and ecology. These components are closely tied to conceptual models (Webster et al., 2003) and nutrient budgets for the estuary (Ford et al., 2003).

Results

The models successfully reproduce observed surface elevation at Lake Creek, salinity and suspended sediment concentrations between the Barrage and the mouth of Fitzroy Estuary, and key features of nitrogen and chlorophyll *a* concentrations.

Results indicate that tidal currents in the estuary are asymmetric and cause fine sediments to be pumped upstream – from the mouth of the estuary towards the Barrage – during periods of low flow. Episodic river flows produce short-term flushing of sediments out of the estuary, however over the annual time scale (for the period modelled), there is a net accumulation of sediment in the estuary. Preliminary scenario

modelling suggests that increasing river discharges would reduce sediment inputs to the estuary from Keppel Bay.

The biogeochemical model shows that the upper estuary is the most productive area of the model domain, with gross primary production exceeding net production by many times. Production in the upper estuary during the low-flow period is fuelled by nitrogen inputs from the sewage treatment plant and meatworks and is limited by low light in the turbid water column. Phytoplankton in the lower estuary appears to be mostly due to downstream advection.

Outcomes and Further Work

This work will feed into continued model development in Stage 2 of the CRC to provide tools, in the form of simulation models and outputs, to facilitate regional planning. The models will be used to assess the likely effects of a number of “what if” scenarios for catchment management. Model development in the next stage will include extending the domain to include Keppel Bay, application of the biogeochemical model to high-flow periods, and a closer examination of denitrification and primary production in the estuary and intertidal mudflats. This will complement field and laboratory studies being conducted as part of the Fitzroy Contaminants (AC) subproject, and the models will be used to guide future monitoring of the estuary.

It is anticipated that the bio-physical understanding and model capability derived here for tropical macrotidal estuaries will be transferable to other similar systems, which are widespread throughout northern Australia, but relatively poorly studied. Through links between this project and other CRC projects, there is an opportunity to use the Fitzroy – Port Curtis region as a case study for the integration of coastal biophysical models with socioeconomic analyses into regional decision-making.

1 Introduction

The Fitzroy is a shallow, macro-tidal estuary in eastern Australia, which discharges into the marine environment at the southern end of the Great Barrier Reef. The major freshwater inflow to the estuary is from the Fitzroy basin, which is the largest catchment in north-eastern Australia. River discharge shows a marked seasonal variation due to rainfall, usually with strong flows from November to May the following year, and dropping almost to zero at other times. The estuarine system can be described as typical of those dominated by summer flood and winter drought discharges in subtropical and tropical Australia (Rochford 1951).

The largest single impact on the estuary ecosystem has been the construction of the Fitzroy Barrage 53 km upstream from the river mouth. This has considerably shortened the estuary and resulted in a loss of habitat and changes to the hydrodynamic character of the lower Fitzroy River, including the creation of a poorly flushed zone downstream of the Barrage (Taylor & Jones, 2000).



Fig. 1.1 Fitzroy Estuary.

With major water infrastructure development undertaken and planned for the Fitzroy, there is need to relate flows and loads resulting from water and land uses to potential impacts on the estuarine system. Limited data indicate average annual sediment delivery to the Fitzroy Estuary is 4 million tonnes with high levels of nutrients and some pesticides (Taylor & Jones, 2000). In order to facilitate understanding of the sediment dynamics in the estuary and provide realistic settings for ecological models, a coupled hydrodynamic - sediment transport model has been developed and applied to the main channel of the Fitzroy Estuary. This model was then coupled with an ecological model, representing biogeochemical processes. The biogeochemical model simulates the transport and transformation of nutrients introduced into the system and their impact on primary production. Nutrients are required for primary production which ultimately represents the foundation for the estuarine

ecology including that of higher organisms such as fish, crustaceans, marine mammals and birds.

This work will feed into continued model development in Stage 2 of the CRC to provide tools and outputs, in the form of simulation models and “what if” scenarios, which will facilitate regional planning. It is anticipated that the bio-physical understanding and model capability derived here for tropical macrotidal estuaries will be transferable to other similar systems, which are widespread throughout northern Australia, but relatively poorly studied. Through links between this project and other CRC projects, there is an opportunity to use the Fitzroy – Port Curtis region as a case study for the integration of coastal biophysical models with socioeconomic analyses into regional decision-making.

This report describes the model calibration process and preliminary results. The limitations of assumptions involved in the calibration and the output from additional model runs are also discussed.

2 Model description and set up

2.1 Model overview

2.1.1 Hydrodynamic and sediment models

Water circulation is modelled using a reduced one-dimensional version of the fine-resolution, three-dimensional, non-linear, non-stationary hydrodynamic model MECO (Model of Estuaries and Coastal Oceans) developed at CSIRO Division of Marine Research (Walker, 1999, Herzfeld, 2003). This model is a general purpose model applicable to scales ranging from estuaries to regional ocean domains. In its application to the Fitzroy Estuary, the model is used to simulate the along-estuary component of current velocity, water level, and salinity distribution.

The predicted currents are used to drive the sediment transport model, which solves an advection-diffusion equation for the mass conservation of suspended and bottom sediments, taking into account the bottom

exchanges by resuspension and deposition (Margvelashvili et al., 2003). The model is one-dimensional and describes sediment concentration distribution and transport of fine sediments in long-estuary directions. It considers the transport of two types of sediment particle within the water column and within a benthic sediment layer. In the latter zone, vertical transport of sediment particles is assumed to occur as a diffusive process through bioturbation. The surface of the sediment layer moves up and down depending whether net deposition or erosion is occurring.

Only cohesive sediment transport is calculated in this study, and the commonly used formula of Ariathurai & Krone (1976) is applied to parameterise sediment resuspension and deposition fluxes. The formulations depend on the specification of bottom stress, which is calculated from the hydrodynamic model. Any feedback between suspended sediment and the density stratification is excluded. The concentration of bottom sediments is simulated assuming no horizontal exchange between adjacent numerical cells. Further, there is no interaction between different sediment classes in the water column. In the sediment bed when fine particles are eroded from the top layer, coarser particles provide armouring of the underlying sediments. The implementation of the model, including the specification of numerical grid, initial data, and lateral boundary conditions, is described in a later section.

2.1.2 Biogeochemical model

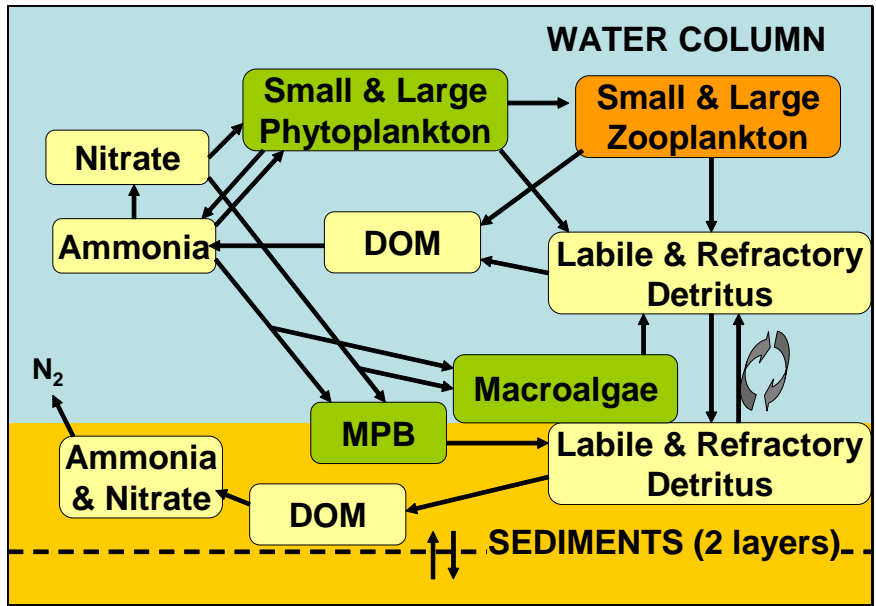


Figure 2.1.1. Major nitrogen pathways in the biogeochemical model.

Simulations were conducted with a biogeochemical model, coupled directly with the one-dimensional hydrodynamic and sediment model (MECOSED) described above. The biogeochemical model simulates the transport and transformation of nutrients introduced into the system as well as primary production. Much of the conceptual development of this model was carried out during the Port Phillip Bay Study (Harris et al. 1996; Murray and Parslow 1997, 1999a, 1999b) however as applied here, the model includes some alterations to customise it for the Fitzroy Estuary. For this application, the model considers the fates of the nutrients nitrogen and carbon. As phosphorus is not considered to be a limiting nutrient in this system, its dynamics were not modelled.

Broadly, the model represents a set of pelagic interactions and a set of benthic interactions controlled by analogous sets of functional groups. As illustrated in Figure 2.1.1, the model may be conceptualised as a series of stores (boxes) and flows (arrows) of nitrogen (or carbon). Some of these flows represent biogeochemical transformations including uptake of nutrients by primary producers, consumption of phytoplankton by zooplankton and organic matter degradation. Coupling the model to MECOSED ensures that physical exchanges – washout to the ocean, burial of organic matter, settling of detritus to the seabed, and diffusion of solutes between water column and sediments – are also represented.

Nitrogen stores in the model include large phytoplankton (diatoms), small phytoplankton (small flagellates), large and small zooplankton groups, microphytobenthos (MPB), macroalgae, nitrogen and carbon in various organic and inorganic forms, and oxygen dynamics. Growth and nutrient uptake by phytoplankton and MPB is represented by a mechanistic model developed by Baird and Emsley (1999). The model employs well-understood relationships for key ecosystem processes and incorporates established literature values for parameters such as maximum growth rates, grazing efficiencies and sinking rates (Murray and Parslow 1997, 1999a, 1999b).

A key feature of the model is its representation of nutrient cycling processes in the sediments. Processes such as benthic organic matter degradation and the return of nutrients to the water column from sediments are particularly important in shallow, energetic systems such as Fitzroy Estuary. Our model adopts the representation of sediment processes used by Murray and Parslow (1997), altered to include two distinct sediment layers – a shallow, active surface layer and a deeper sediment store. This representation is effectively the type 3 representation described by Soetart et al. (2000), in that it is sufficiently complex that it describes the major processes occurring within sediments in a semi-empirical way, but it is not a fully depth-resolved diagenesis model.

Intertidal mudflat areas are extensive in macrotidal systems like the Fitzroy Estuary. These areas can make a significant contribution overall production and nutrient exchanges. Microphytobenthos in the intertidal zone have been found to account for as much as 50% of total primary production in some estuaries (MacIntyre and Cullen 1996; Goto et al., 2000). To properly represent microphytobenthos, a model must be able to account for these intertidal areas, which vary in size along the length of the estuary with the slope of the banks and the magnitude of tidal surface level variations. For the present application, we therefore included a new algorithm in the model that allows variations in light climate across the width of the river channel to be taken into account within the context of a one-dimensional (longitudinal) model. This is important because it allows

a more accurate simulation of growth of microphytobenthos on intertidal mudflats.

2.2 Numerical grid

The modelling domain is 80 km long, stretching from the Fitzroy Barrage along the main channel and well into the sea. The first 53 cells of the numerical grid are within the estuary at 1 km intervals. The last 27 cells from the sea side are set to obtain a salinity boundary condition at the mouth that does not rely on interpolation between monthly monitoring data. A side channel of 4 cells connecting to the main stem of the estuary represents the Loop in the middle estuary (Fig. 1.1). The main channel is set as passing through the cut-through. Note that distances here and in the following report are all measured as downstream from the Barrage at Rockhampton.

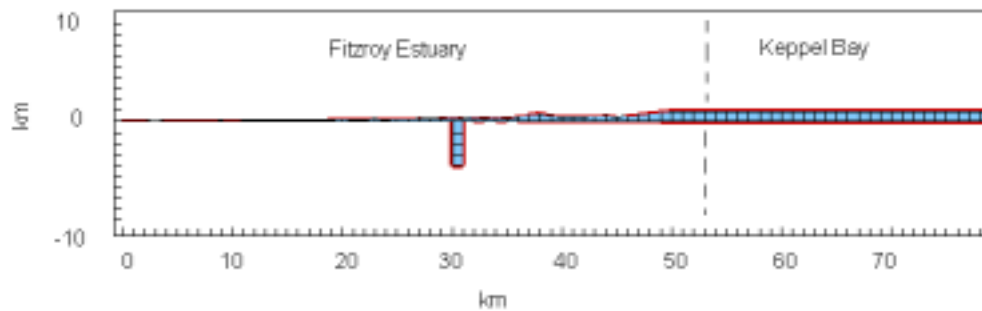


Fig 2.2.1 The numerical grid.

Because the model allows only rectangular cells in cross-section, it does not account for the variation in channel width with water level. The cell widths have been set equal to the river width at mean water level multiplied by a constant coefficient, while the cell depths were calculated from the cell widths and known cross-section areas along the main channel. The width coefficient has been used as a calibration parameter to provide a better match between observed and measured surface elevation at Lakes Creek near the head of the estuary.

The horizontal resolution of the sediment bed is the same as the resolution of the water column. There are two layers of sediment in the model, including an active upper layer with a constant thickness of 5 mm,

and an underlying layer of time varying thickness. The initial thickness of the sediment bed is set to 20 cm.

2.3 Initial data and forcing

The model requires a prescribed initial condition as well as the specification of seaward and landward boundary conditions as it progresses through time. At the upstream boundary, the hydrodynamic module is forced with known river flow at the Barrage (Fig. 2.3.1) having zero salinity. The surface elevation as measured at Port Alma, zero-gradient condition for the velocity, and a constant salinity of 36.5 psu are the boundary conditions specified at the seaward end of the model domain, 80km downstream from the Barrage.

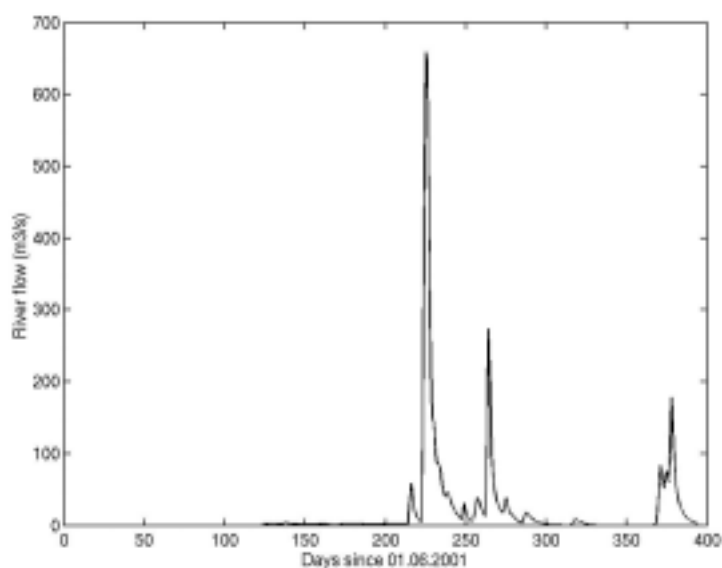


Fig. 2.3.1 River flow at the Barrage.

Estuarine sediments are mixtures of particles with different grain sizes. Modelling of such mixtures on the scale of the whole estuary is currently still in a preliminary state, mainly because of lack of data required to initialise, run and calibrate models. In practice, simulations are carried out using as small number of sediment classes as possible. Often, a very limited number of sediment fractions suffice to obtain reasonably good matches between model and data (Teeter et al, 2001). In the Fitzroy

Estuary the best match between model and data has been achieved using three classes of sediments, representing estuarine particles, river sediments, and an unerodible fraction of coarse, bottom sediments. Both estuarine and river sediments are cohesive but are assumed to have different initial distributions, boundary conditions, and settling velocities. Considering that old estuarine deposits and fresh river loads could have different physical and chemical properties, this subdivision seems justified.

It is assumed that there are no river sediments in the estuary, until they are discharged from the Barrage. (Fig. 2.3.2 a), and there is no input of estuarine particles through the upstream boundary. At the seaward boundary, a free-flow boundary condition is applied to all sediment fractions when the flow direction is out of the computational domain. During the inflow at the seaward end, small background values of sediment concentrations are specified at the boundary.

When the modelled river sediments enter the estuary, they flocculate in salty water and increase their settling velocity from 10^{-5} to $3 \times 10^{-4} \text{ ms}^{-1}$. The settling velocities for estuarine sediments are specified as $5 \times 10^{-4} \text{ ms}^{-1}$ in fresh water and $8 \times 10^{-4} \text{ ms}^{-1}$ in salty water. The calculated settling velocities linearly increase with salinity. Sediment particles are unflocculated in fresh water and flocculation is complete when the water salinity reaches 5 psu. Optimal sediment settling velocities and flocculation regime are derived from the model calibration runs.

First, a preliminary run of 6-month duration is carried out to allow the adjustment of the distribution patterns in bottom sediments to hydrodynamic forcing. The 6-month model run is initialised with zero concentration of sediments in the water column. In the sediment bed, initial concentrations are 600 kg m^{-3} for estuarine particles, and 600 kg m^{-3} for the unerodible fraction of sediments

Because of the strong coupling of the estuary with the adjacent sea, the sediment fluxes through the mouth of the estuary are sensitive to the

hydrodynamic and transport conditions in the open coastal area outside the estuary. The simple extension of the model domain from the estuary mouth at $x = 53$ km to the offshore model boundary at $x = 80$ km appears to have provided a satisfactory salinity boundary condition, but this has proved to be less satisfactory for the sediment simulations. Limited data from monthly observations obtained by the Queensland EPA show increased concentration of suspended solids in the lower estuary in the summer season and less sediment suspended in the water column in winter (Fig. 2.3.2 b)

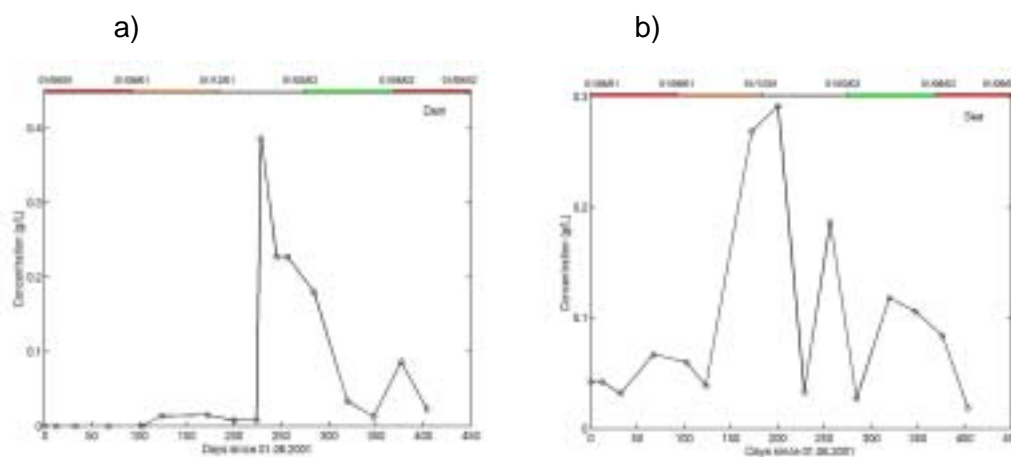


Fig. 2.3.2 Linearly interpolated monthly sediment concentration at the Barrage (a) and at the mouth of the estuary (b).

This could be indicative of seasonal variability of the suspended sediment concentrations in the lower estuary and Keppel Bay. For example, the summer intensification of rainfall (Fig. 2.3.3) could drive enhanced erosion of sediments from the banks and mud flats. Wind driven waves and currents (Fig. 2.3.4) could be causing long-term redistribution of sediments in Keppel Bay and in the estuarine mouth.

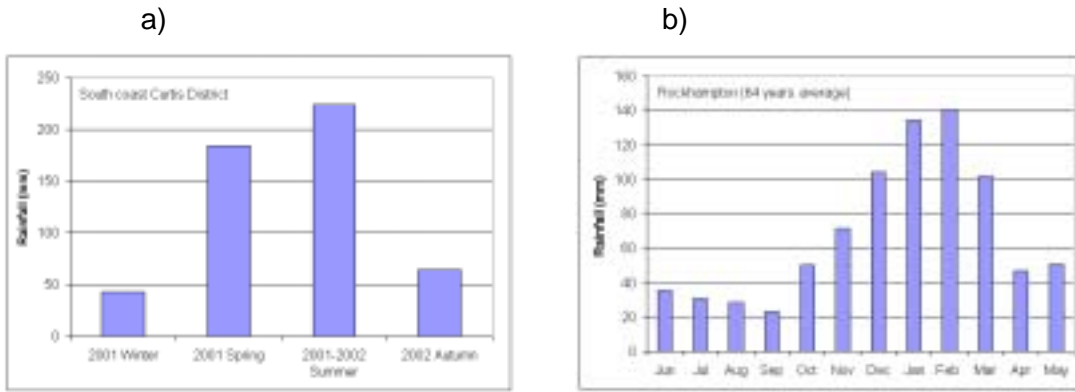


Fig. 2.3.3 Rainfall (a) averaged over South Coast Curtis District (Annual water statistics, 2001-2002) (b) averaged over 64 years, Rockhampton (BoM).

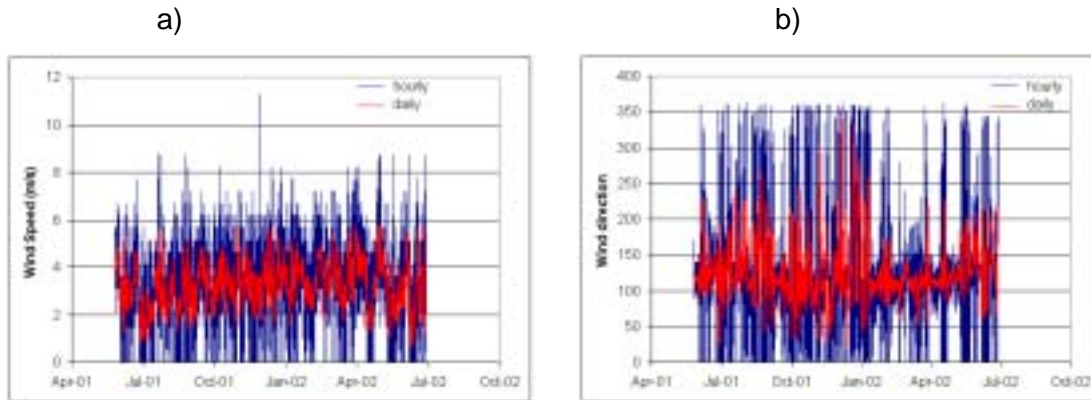


Fig. 2.3.4 Wind speed (a) and direction (b) in Rockhampton (BoM).

Neither wind-driven circulation nor rain-driven erosion of sediments from the mud flats are simulated in this study. To mimic concentrations at the mouth of the estuary, the calculated sediment concentrations at the lower limit of the estuary are relaxed to the interpolated monthly monitoring data using the following formula:

$$\frac{\partial C}{\partial t} = Advection + Diffusion + Resuspension / Deposition + \alpha(\hat{C} - C)$$

The last term in the right hand side of this equation represents point sink/sources, added to the transport equation in order to relax the calculated sediment concentrations (C), to the measured concentrations (\hat{C}); α is the relaxation rate constant. This approach enables us to calculate instantaneous tidally driven resuspension and deposition which

causes significant semi-diurnal fluctuations in suspended sediment concentrations while forcing the overall sediment concentrations to follow the more slowly varying seasonal trends. An example of simulated sediment concentrations at the estuarine mouth is given in Fig. 2.3.5.

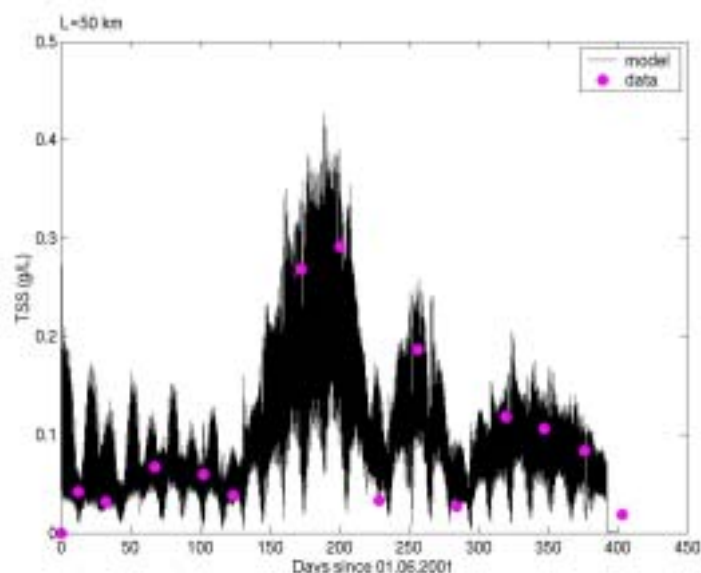


Fig.2.3.5 Calculated and monthly measured sediment concentrations at the mouth of the estuary. The thick black line represents the variation due to tidal oscillations in the numerical solution, while the red dots show concentrations as measured during the monthly monitoring program

The model basic parameters (Table A1 in the Appendix), as well as initial concentrations of the sediment fractions and the settling velocities, have been derived from the model calibration runs. Parameter values used with the biogeochemical model are given in Table A2.

Several additional assumptions are made for the simulations of sediment transport in the Fitzroy Estuary. Firstly, due to the large tides and vigorous tidal currents, the wind impact on the hydrodynamics and sediment transport has been neglected. Secondly, only transport of cohesive sediments has been simulated and no account for bed load transport is made. Thirdly, because of the lack of suitable calibration/verification data, sediment consolidation is not simulated.

The model grid and hydrodynamic parameter values for the biogeochemical model were the same as that used for the sediment modelling. All inflow and tidal boundary conditions, as well as boundary

concentrations of suspended solids and meteorological conditions, were also specified as described previously.

At the downstream boundary, water flowing into the domain on a flood tide was assumed to have a nitrate concentration of 0.1 mg L^{-1} and an ammonium concentration of zero. These values were taken from observations in the lower estuary when salinity exceeded 30 psu and hence are representative of concentrations in incoming marine water. Boundary conditions at the open tidal boundary for concentrations of other tracers were set according to the furthest downstream measured values where measurements were available.

For water flowing into the estuary from the upstream boundary (at the Barrage), phytoplankton concentrations were assumed to be zero. At this upstream boundary, nitrogen concentrations were set according to nominal river concentrations calculated from the nutrient budgets reported by Ford et al. (2003) and concentrations of other tracers were set to match observed concentrations at the furthest upstream sampling site within the estuary.

2.3.1 Point sources

Two point sources of nitrogen were represented within the model. Nitrate, ammonium, dissolved organic nitrogen and detrital nitrogen inputs from the sewage treatment plant and from the meatworks were derived from the nitrogen budgets for the estuary. Inputs from the sewage treatment plant were assumed to enter the estuary in the area between 12.5 and 16.5 km downstream of the Barrage, while inputs from the meatworks were added between 16.5 and 23.5 km downstream of the Barrage. These areas correspond to box 2 and box 3 respectively in the model used to determine nutrient budgets.

Nominal river nitrogen concentrations (mg N m^{-3}) and loads from point sources (kg N day^{-1}) were held constant between sampling dates.

3 Model simulations

3.1 Hydrodynamics

The hydrodynamic model was calibrated in two stages. During the first stage, it was calibrated by adjusting the width coefficient and bottom drag coefficient to match the observed elevation at Lakes Creek towards the landward end of the estuary. Despite the coarse model geometry, it was possible to achieve a good match between model and data (Fig. 3.11). Note that the measured elevations have been clipped for water elevations below -1.2m due to the sensor coming out of the water.

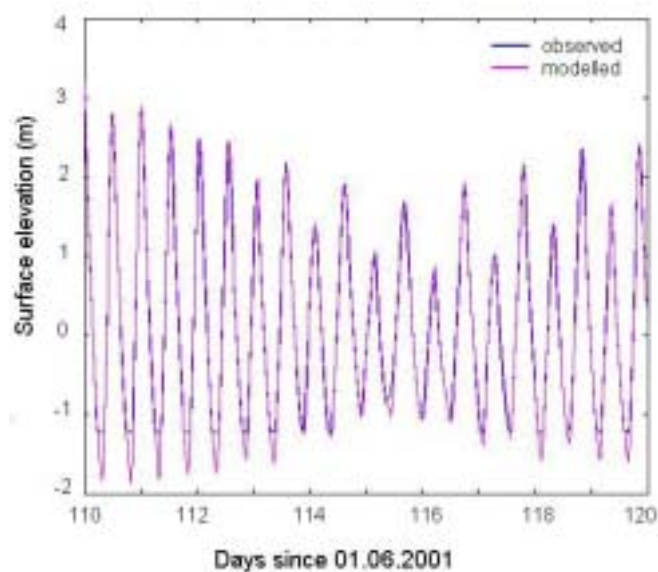


Fig. 3.1.1 Modelled and calculated surface elevation at Lakes Creek.

To optimise the match with observed salinities along the estuary, a number of advection schemes were tried along with different diffusion coefficients. The best result was achieved by using a first-order upwind advection scheme with the long-estuary diffusion coefficient set to zero, so that any horizontal mixing in the model was driven only by numerical diffusion (Fig. 3.1.2).

Comparing model performance with observations, it seems probable that there was some discrepancy between the river discharge prescribed in the model and actual freshwater input to the estuary. For example, the river flow data used in the model show a small but consistent flow of $1\text{-}3\text{ m}^3\text{s}^{-1}$ in the period between 124 and 215 days since 1 June 2001, while observations do not exhibit any drop in salinity near the Barrage during

this period. In fact, it seems that during this time much of the river flow measured at the Gap was diverted to refill a reservoir upstream from the Barrage. Other visual discrepancies can be attributed to a scarcity of measurements that are not able to resolve changes in the system that occur on short timescales such as those due to flow events. Note that the interpolated observations shown in Fig. 3.1.2 are derived from the data obtained at fixed times and fixed positions along estuary, and did not account for the back and forward motion of the isohalines with the tide.

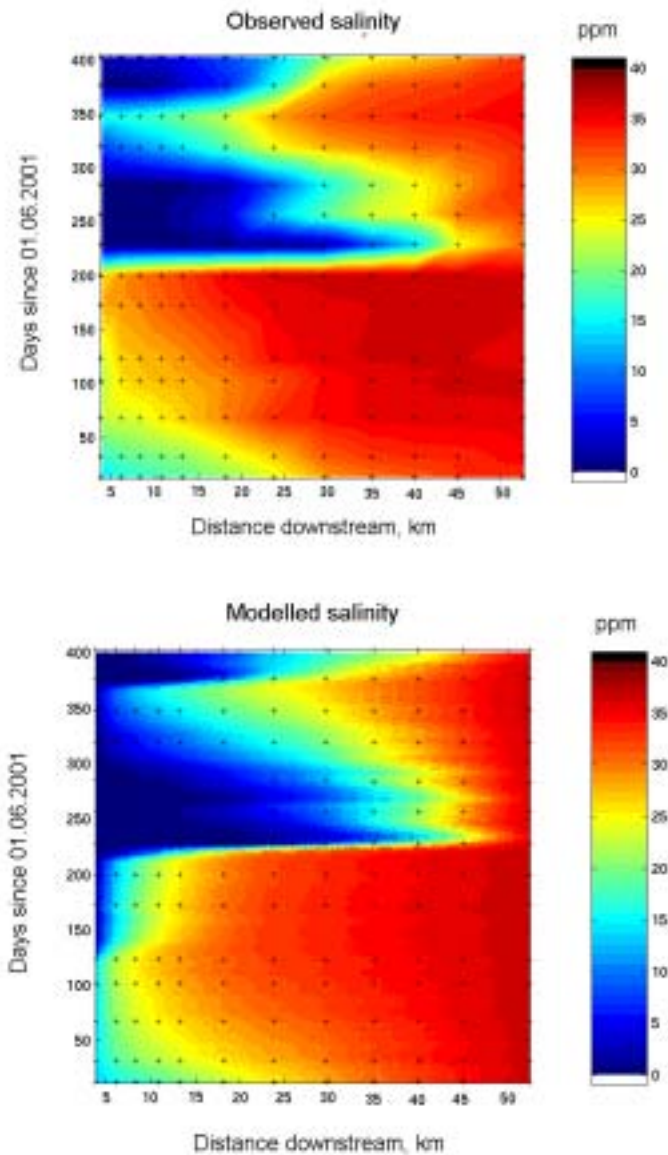


Fig. 3.1.2 Modelled and measured salinities. The “+” markers on the upper chart for the observed salinity show the times and locations of the measurements. The lower chart shows modelled salinities, which have been averaged to remove the semi-diurnal and diurnal tidal variations.

As tides enter the estuary, they undergo considerable modification. Friction with the sides and bottom of the channel causes energy and amplitude loss, while a decrease in cross section upstream along the estuary causes energy concentration and an increase in amplitude as the tide propagates upstream. According to the simulations in the Fitzroy Estuary, the tidal excursion of surface elevation increases with distance upstream along the estuary (Fig. 3.1.3 a), while the tidal currents undergo substantial attenuation and reach minimum values at the Barrage (Fig. 3.1.3 b).

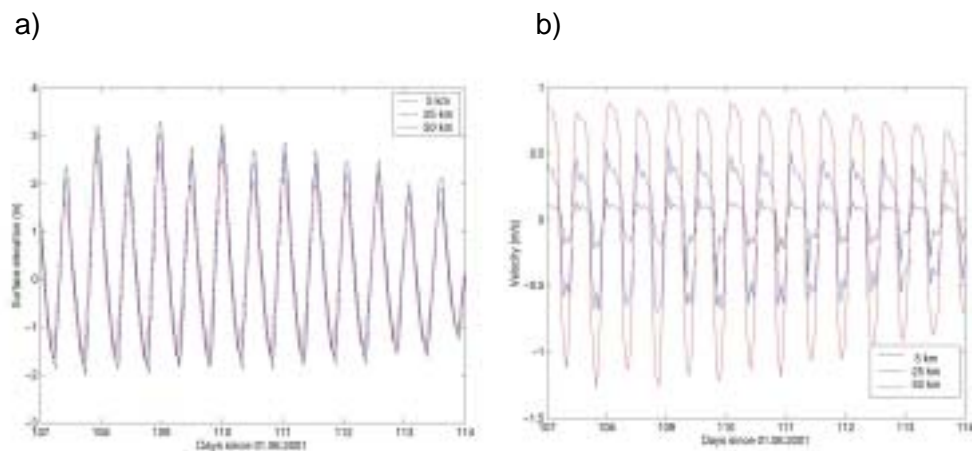


Fig. 3.1.3 Calculated surface elevation (a) and velocity (b) at different distances from the Barrage.

Water depths along the estuarine channel do not appreciably exceed the tide amplitude so that the ratio of water depths under high and low tides may be substantially greater than 1. Consequently, the speed of propagation of the tidal wave may be substantially greater under the crest of the tidal wave than under its trough so that the crest tends to overtake the trough. This produces an asymmetric tidal wave with a shortened duration of flood and a lengthened duration of ebb. This effect is accompanied also by an asymmetry of tidal current velocities: flood velocities are increased, whereas ebb velocities are decreased (Fig. 3.1.3 b).

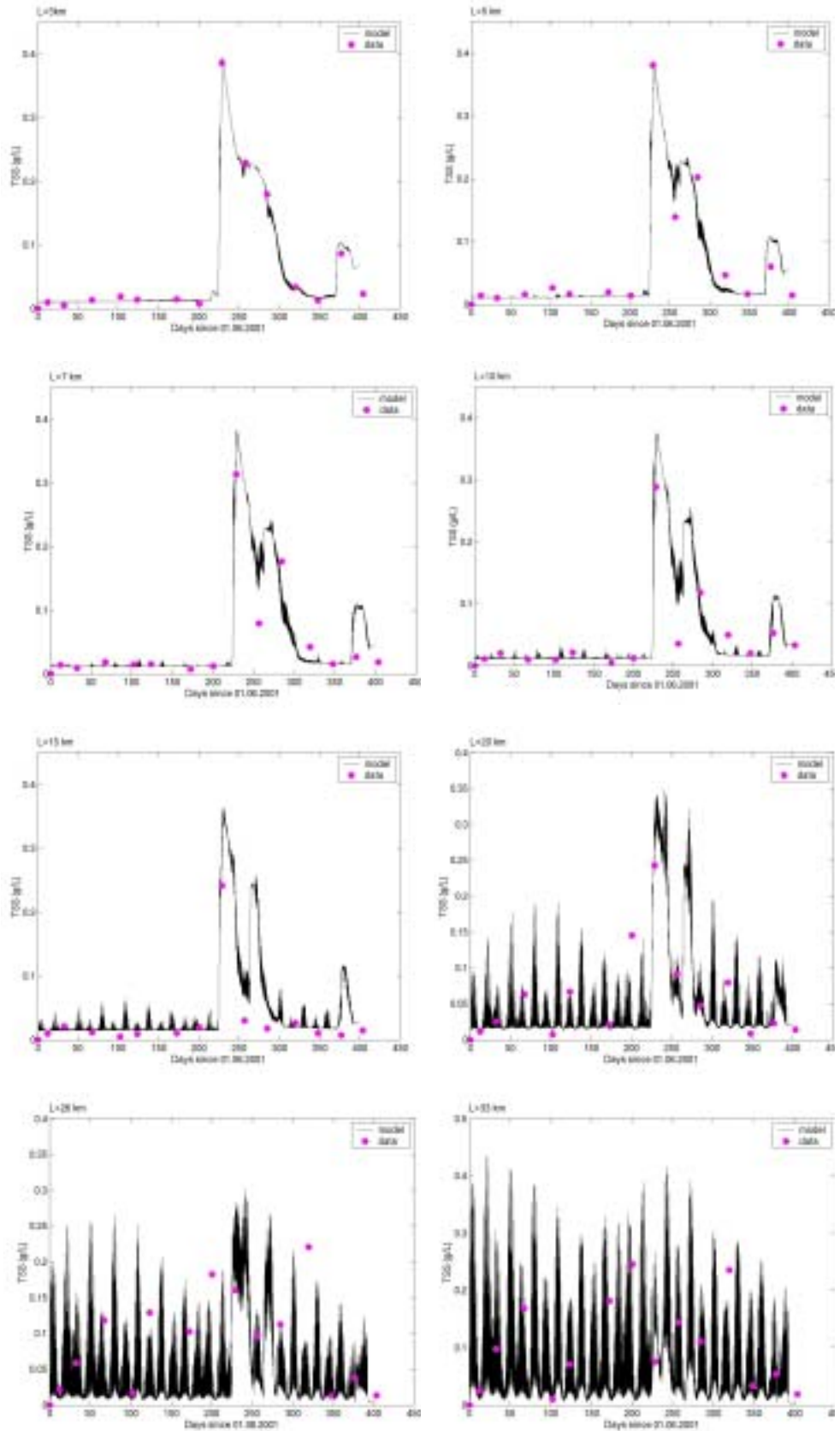
3.2 Sediments

3.2.1 Sediment model vs observations

Calculated concentrations of the suspended solids and monthly monitoring data are compared in Fig. 3.2.1. According to the measurements, unless there are significant water flow and sediment loads through the Barrage, the concentrations of suspended solids in the lower part of the estuary are higher than those upstream. For example, the concentration of suspended sediments within 20km of the Barrage (upper estuary) is typically less than 0.04 g/L, while the tidally driven resuspension and advection in the lower estuary (below 30km) causes concentrations of sediments to vary between $\sim 0.01 \text{ g L}^{-1}$ and up to 0.3 g L^{-1} . The elevated discharge event between 224 to 231 days caused concentrations of suspended solids in the upper estuary to reach $\sim 0.4 \text{ g L}^{-1}$.

In agreement with observations, the model predicts lower sediment concentrations in the upper estuary (typical values less than 0.04 g L^{-1}) and the concentrations in the lower estuary to range between 0.01 and 0.5 g L^{-1} . Note that in the lower estuary, the predicted suspended sediment concentration is very dependent on tidal phase with highest concentrations tending to occur during the time of greatest flow speed (Fig 3.2.2). In the upper estuary, because of less energetic tidal currents, the interplay between advection, resuspension and flocculation results in a more gradual evolution of the concentration curves, which is quite well reproduced by the model. At 3 km distance downstream from the Barrage, the simulated concentrations, as expected, are close to those specified at the upstream boundary (Fig. 2.3.2a). Further downstream ($x = 5 - 20 \text{ km}$), during the flow events between 250 to 300 days, the concentration curves undergo non-monotonic variations with the rapid decline of the sediment concentrations at ~ 250 to 260 days being caused by salinity enhanced flocculation and settling.

FITZROY NUMERICAL MODELS



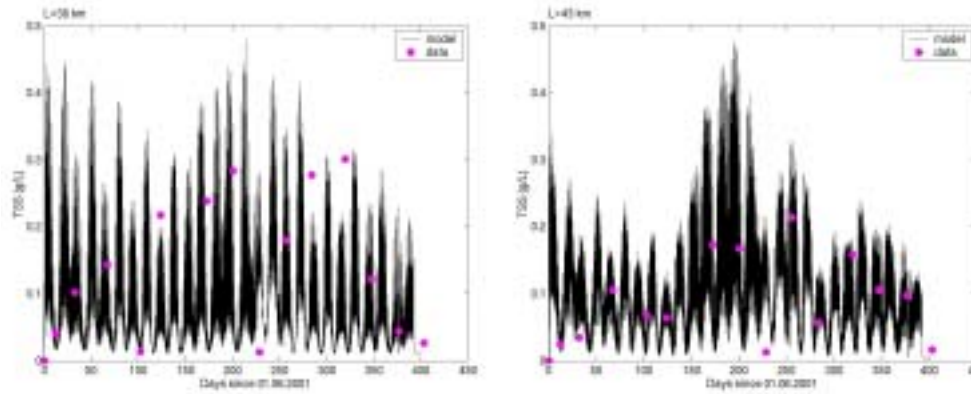


Fig. 3.2.1 Modelled concentrations of suspended sediments vs. monthly monitoring data.

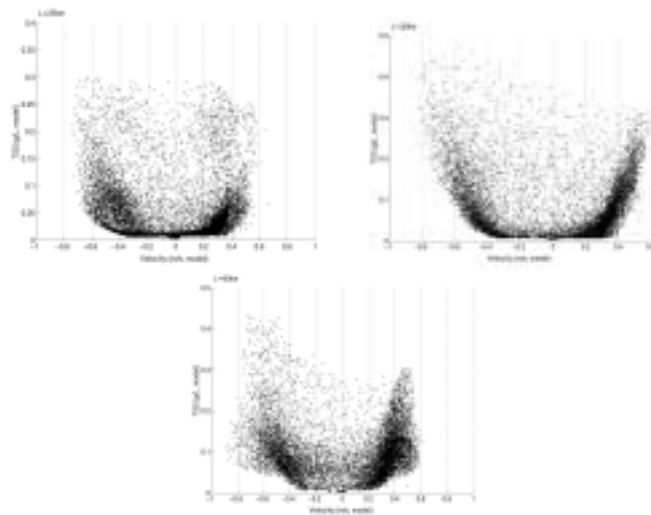


Fig. 3.2.2 Modelled concentrations of TSS vs. simulated river velocities.

The model performance is illustrated also in Fig. 3.2.3, where the calculations are plotted against all available monthly monitoring data for TSS. From Fig 3.2.1 and 3.2.3 it appears that the model reproduces general patterns and trends in the sediment distribution in the Fitzroy Estuary, although there are substantial discrepancies between individual measurements and modelled TSS in the lower, most energetic part of the estuary. In this respect, it should be noted that the calibration process involves adjusting the model to reproduce known behaviour with an acceptable degree of precision. During this process, the limitations applying to the accuracy of the available data need to be kept in mind.

In a macro-tidal estuary, the interpretation of the results from the usual monthly monitoring program is difficult because of the large variation of

individual measurements associated with turbulent fluctuations of suspended sediment concentrations. Such fluctuations are often measured and observed as small-scale turbidity plumes appearing at the water surface with spatial scales ranging from a few meters to several hundred meters. Short-term (tidal-scale) variations in TSS concentrations of a factor of two have been measured in the Ord Estuary during an ongoing research study (Parslow et al. 2003). In the Brisbane River, considerable spatial variation of turbidity associated with the development of the turbidity plumes during the flood events has been reported (Howes, et al., 2003). Such small-scale variability of suspended sediment concentration is likely to be present in the Fitzroy Estuary as well. Given these fluctuations and taking into account lack of data to specify tide-resolving boundary conditions at the estuarine mouth, the agreement between model and measurements, illustrated in Figs. 3.2.1 and 3.2.3, should be considered to be reasonably good. The model is capable of reproducing the major features of the spatial and temporal variation of the suspended sediment distribution in the Fitzroy Estuary

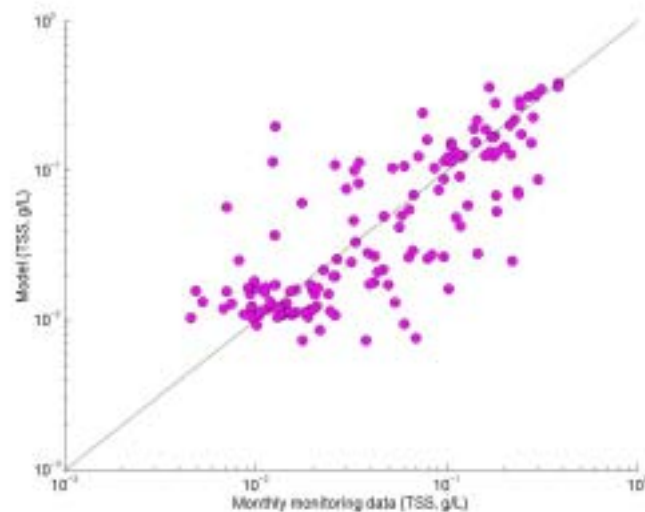


Fig. 3.2.3 Modelled concentrations of suspended sediments vs. monthly monitoring data.

The contribution of the simulated river loads to suspended concentrations in the estuary at different distances from the Barrage is illustrated in Fig. 3.2.4. In the upper estuary during the time of peak flood, the concentration of river sediments exceeds the concentration of

resuspended estuarine sediments by a factor of about two, while at 40 km downstream from the Barrage, suspended sediments are predominantly estuarine.

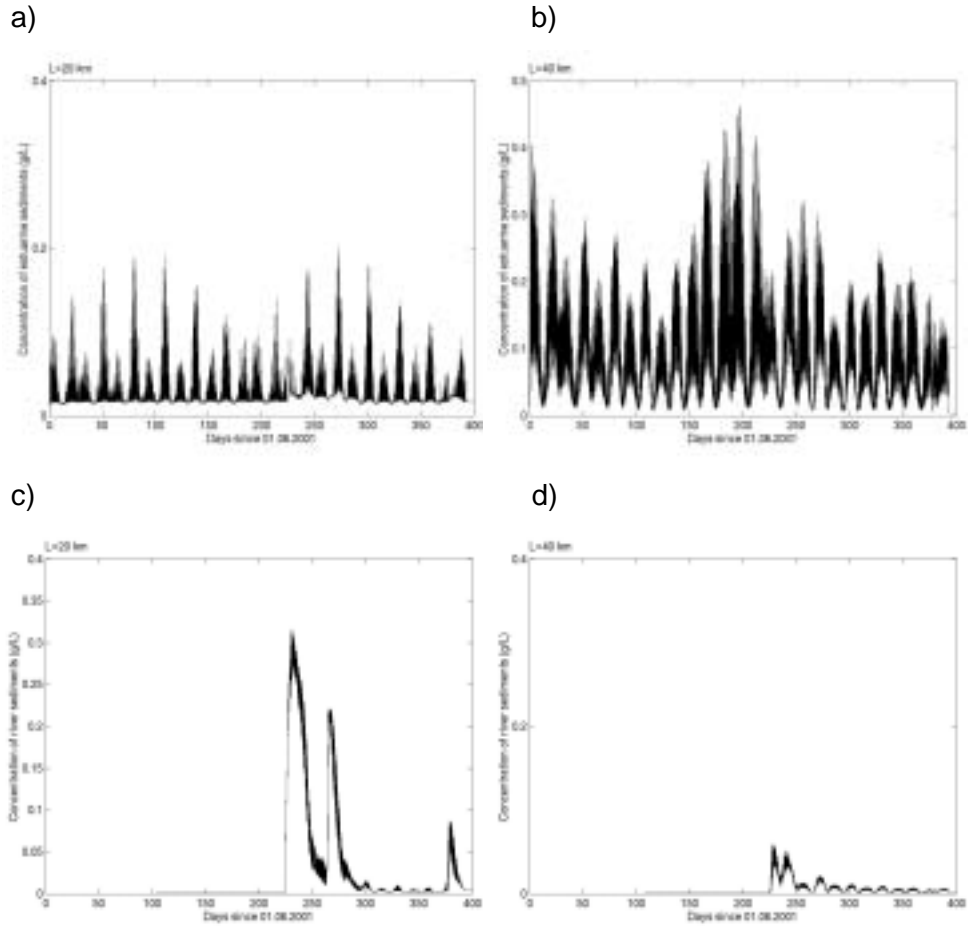


Fig. 3.2.4 Calculated concentrations of river sediments at different distances from the Barrage. (a),(b) - estuarine sediments; (c),(d) - river particles.

In order to evaluate the impact of salinity-induced flocculation on the sediment distribution in the estuary, additional simulations have been carried out assuming no flocculation of fine sediments. These simulations, illustrated in Fig. 3.2.5, show a large discrepancy between model and measurements when sediment flocculation is neglected. Compared to the results with flocculation shown in Fig. 3.2.1e, the suspended sediment concentrations remain elevated far too long following the flow event of 224-240 days. It would seem that flocculation is an important part of fine sediment dynamics in the Fitzroy Estuary.

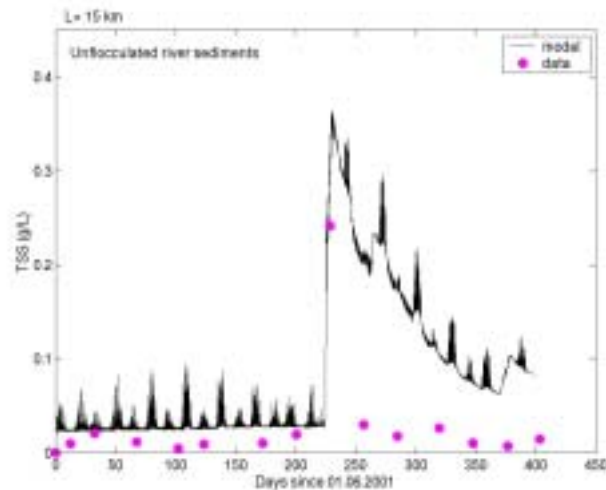


Fig. 3.2.5 Concentration of suspended sediments predicted when flocculation of river sediments is neglected.

3.2.2 Sediment redistribution and fluxes

The simulated distribution of suspended sediments in the estuary over the whole simulation period is presented in Fig. 3.2.6. For much of the time, particularly in winter, tidal resuspension processes tend to cause the highest suspended sediment concentrations to occur in the section of the estuary between $x = 30 - 40$ km. However, there are marked temporal changes in the distribution patterns due to the spring-neap cycle of tidal amplitudes and to the assumed seasonal variability of the sediment concentrations at the estuary mouth. Also, the elevated concentrations associated with the river inflow events (224-300 days) are clearly evident. During the summer season, the concentration of sediments in the open coastal water increases, and the maximum in suspended sediment concentration shifts toward the mouth of the estuary.

The small discontinuity in along-estuary sediment distribution at 30 km downstream from the Barrage near the Loop (Fig. 3.2.6) is caused by the increased area of this cross section that reduces current velocities in this part of the estuary. Reduced currents and shear stresses result in intensive sediment deposition and low concentrations of particles suspended in the water column.

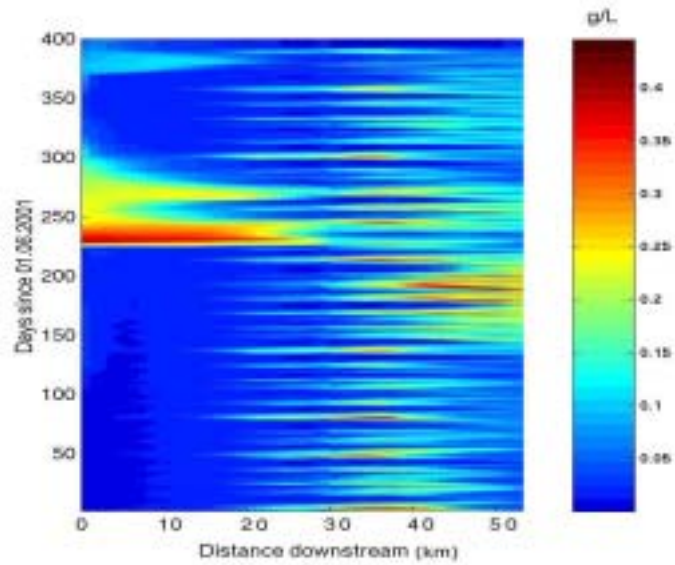


Fig. 3.2.6 Calculated concentrations of TSS.

The time series of friction velocities computed from the hydrodynamic model for sites in the upper and lower estuary are shown in Fig. 3.2.7. For fine-sediment resuspension to occur, the specified critical friction velocity must be exceeded. This critical friction velocity is shown as a red line in the figure. This threshold is only occasionally exceeded in the uppermost section of the estuary during high river flow, but it is almost always exceeded during some part of the tidal cycle in the lower estuary.

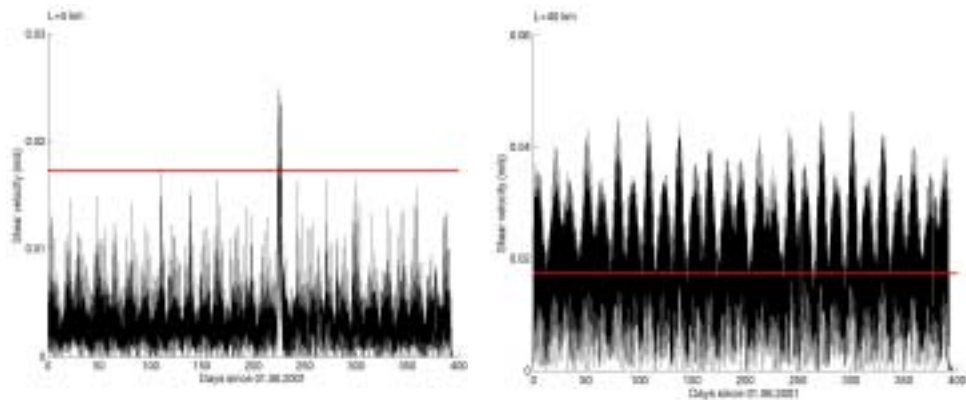


Fig. 3.2.7 Modelled bottom shear velocities.

The high variability of the shear stresses along the estuary is illustrated in Fig. 3.2.8, where calculated shear velocities during one tidal cycle (neap tide) are depicted. Friction velocities tend to increase downstream from the Barrage to the mouth of the Fitzroy. Local departures from a

monotonic increase are due to variations in channel cross-sectional area, which cause local variation in tidal current velocity. Localised minima of friction velocity are likely to represent sediment deposition sites where resuspension of settled sediments is less vigorous.

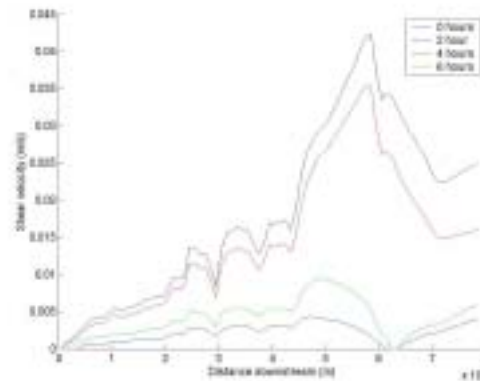


Fig. 3.2.8 Modelled bottom shear velocities along estuary.

During low or zero river flows, the upstream and downstream transport of water during the flooding and ebbing phases of the tidal cycle are approximately balanced. However, sediment transport depends on the amount by which the velocity exceeds the threshold velocity necessary to initiate sediment resuspension and motion. In asymmetric flow, sediment fractions with a critical resuspension velocity greater than the ebb velocities, but less than the flood velocities, are resuspended during the flood and remain settled on the bottom during the ebb. The net result of such asymmetry is pumping of fine sediments into the estuary and up-estuary towards its head. This is illustrated in Fig. 3.2.9 where the simulated redistribution of bottom sediments in the top sediment layer is depicted. Because of the upstream pumping of sediments, the relatively coarse estuarine sediments accumulate within 23 km of the Barrage. There are also localised spots of intensive deposition in the middle estuary. Maximum accumulation of the finer riverine particles also occurs in the upper estuary. Fresh deposits of fines are partially mixed deeply into the benthic sediments by bioturbation and partially washed out of the estuary during high river flow.

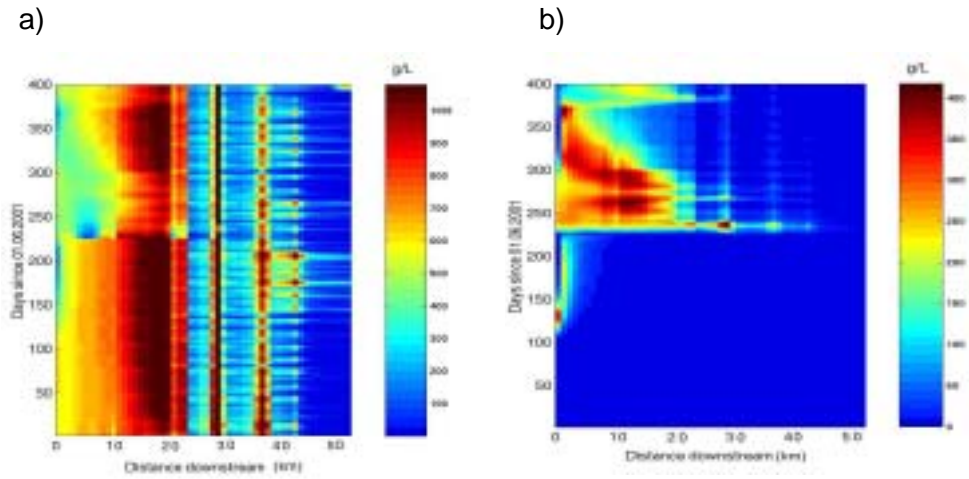


Fig. 3.2.9 Concentration of sediments in the top sediment layer. (a – estuarine sediments, b – river sediments).

The simulated redistribution of the sediment thickness after 400 days is shown in Fig. 3.2.10. Key features are predictions of a 90 cm increase in sediment thickness near the Loop, the accumulation of sediments in the upper estuary, and the dominance of sediment erosion through the lower estuary.

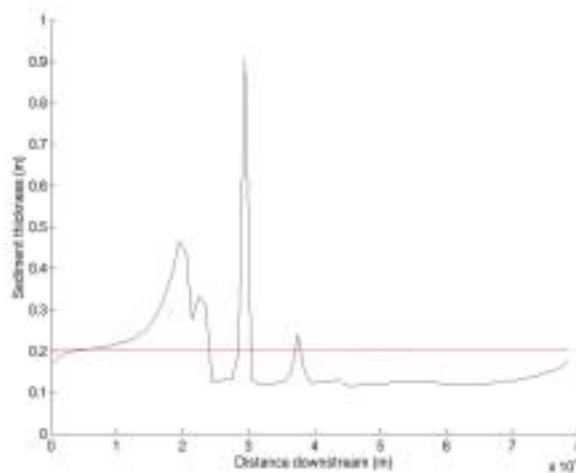


Fig. 3.2.10 Modelled sediment thickness along estuary after 400 days of simulation.

Fig. 3.2.11 shows the time series of the simulated sediment flux through the mouth of the estuary (x=50 km). The large temporal variability in the flux occurs at time scales ranging from that associated with the semi-diurnal fluctuation of the tides (period ~6 hours), through the spring-neap cycle (period ~14 days), to seasonal timescales.

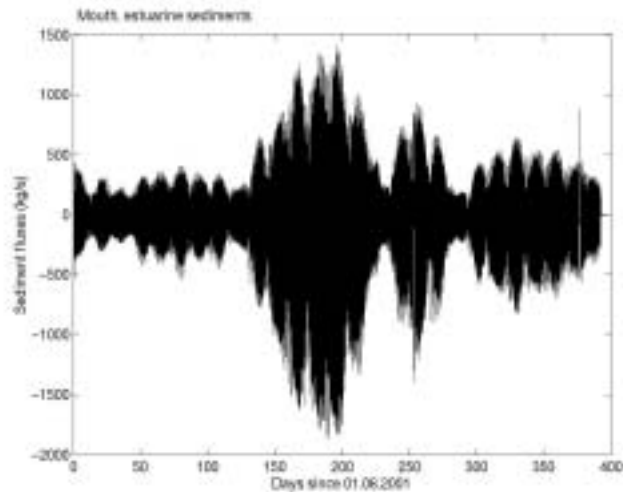


Fig. 3.2.11 Sediment fluxes at the mouth of the estuary (estuarine particles).

In Fig 3.2.12, estuarine sediment fluxes at the mouth of the estuary, modelled for an elevated river flow regime, are compared to those modelled using the measured river flows (the base scenario). Both scenarios use the same initial and sea-boundary conditions as for the analysis already described. For the scenario involving elevated river discharges, the river flow is the measured river flow increased by a factor of three, as is the input load of TSS through the Barrage. Modelling based on such an idealised scenario is used to illustrate how river flow impacts on the estuarine sediment transport.

To simplify the analysis of the model output, instant horizontal fluxes of estuarine sediments are integrated over the simulation time:

$$F(t) = \int_0^t f(t)dt$$

Here $f(t)$ is an instant sediment flux given in (kg s^{-1}), while $F(t)$, given in (kg), is the mass of sediment transported through the cross-section accumulated from the beginning of the simulations up to the time t .

When $F(t)$, which is calculated at the mouth of the estuary, increases with time, sediments are being discharged from the estuary; sediment accumulates in the estuary when $F(t)$ decreases with time.

Over the whole period of the simulations, both the base scenario and the elevated flow scenario show a net influx of coarser estuarine sediment into the estuary (Fig. 3.2.12). For the elevated flow scenario with three times the river discharge, the net sediment accumulation within the estuary is reduced by a factor of about 3. During the winter season with low sediment concentrations at the seaward boundary, the estuary discharges sediments to the sea, while during the summer season sediments are delivered into the estuary from the coastal area beyond its mouth. For both scenarios, the high flow events (224-300 days) produce short-term discharge of sediments from the estuary. However, over the annual time scale, the net balance between sediment pumping upstream and flushing out of the estuary is the accumulation of sediments in the estuary.

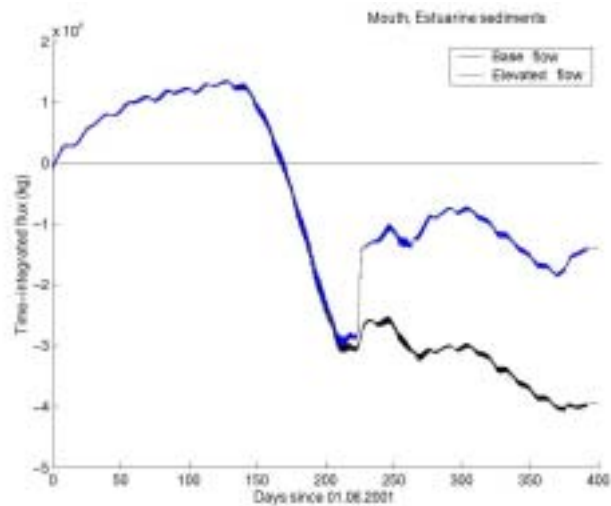


Fig. 3.2.12 Integrated sediment fluxes at the mouth of the estuary for the base and elevated flow scenarios (estuarine particles).

Down-estuary transport of the fine river sediments under the base and elevated flow scenarios are illustrated in Fig. 3.2.13. Because of less effective pumping of fine particles by asymmetric currents and the low concentration of river sediments in the open coastal waters, river sediments are discharged to the ocean. However, the net balance between river input through the Barrage and sediment discharge to Keppel Bay is the accumulation of particles within the estuary. More than 90% of the total input of river sediments accumulates in the estuary during the base scenario flows. Increasing the river flow by a factor of

three reduces the fine sediment accumulation within the estuary to ~35% of the total input.

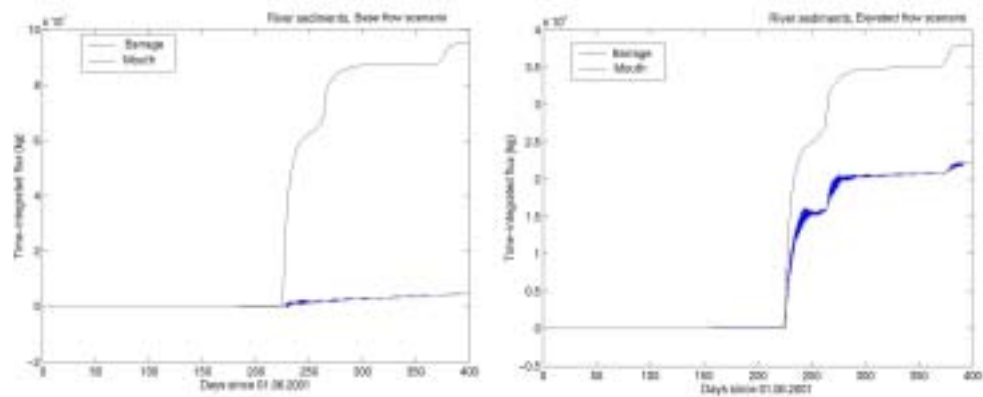


Fig. 3.2.13 Integrated sediment transport for the base and elevated flow scenarios (river sediment).

The calculated accumulation of sediments in the Fitzroy Estuary for the base and elevated flow scenarios are presented in table 3.2.1.

Table 3.2.1 Modelled accumulation of sediments in the Fitzroy Estuary for the base and elevated flow scenarios.

Scenario	Accumulation of river sediments (kT)	Sediment input through the estuarine mouth (kT)
Base flow	85	400
Elevated flow	160	140

3.3 Biogeochemistry

The dynamic biogeochemical simulation model was calibrated to reproduce observed nitrogen concentrations and chlorophyll *a* during the low-flow period, a 250-day period between 22 April and the end of December 2001. This period was chosen because, as discussed in the conceptual model for the estuary, it is during periods of low flow (and hence higher residence times) that biogeochemical transformations within the estuary are most significant to the ecology of the estuary. This was also the period for which the most comprehensive field data for a range of variables, including light extinction within the water column, were available.

Observed and simulated nitrate + nitrite (NO_x) concentrations and total nitrogen concentrations are illustrated in Figures 3.3.1 and 3.3.2. In each case, daily model output is shown, together with model output subsampled to show model results interpolated between the dates on which observations were made. This illustrates how sampling procedures can alias data and affect interpretation of results, especially in a macrotidal system.

In general, the model reproduces observed nitrate and total nitrogen moderately well, however, peak nitrate concentrations are somewhat over-estimated and simulated nitrate maxima appear to occur several days early. This may be due to the assumption that inputs from all external sources are constant between one sampling date and the next. The exact timing of inputs relative to freshwater inflows and spring and neap tides may affect the efficiency with which processes within the estuary remove nitrogen from the system. Further calibration of the model may also be required.

Nitrate and total nitrogen concentrations are generally considerably higher near the Barrage than further downstream. Nitrogen is removed from the water column within the estuary by denitrification and by uptake by diatoms, which subsequently settle into the sediments. More importantly, however, nitrogen concentrations in the lower estuary are

reduced by tidal mixing and dilution with low-nitrogen marine water. Periods in which nitrate concentrations near the Barrage are relatively low (e.g. day around day 540 and day 670) correspond with periods in which uptake by phytoplankton (reflected in chlorophyll a concentrations, Fig. 4) is high. As chlorophyll a concentrations fall, nitrate concentrations are quickly restored due to continuous inputs to the upper estuary from the sewage treatment plant and meatworks.

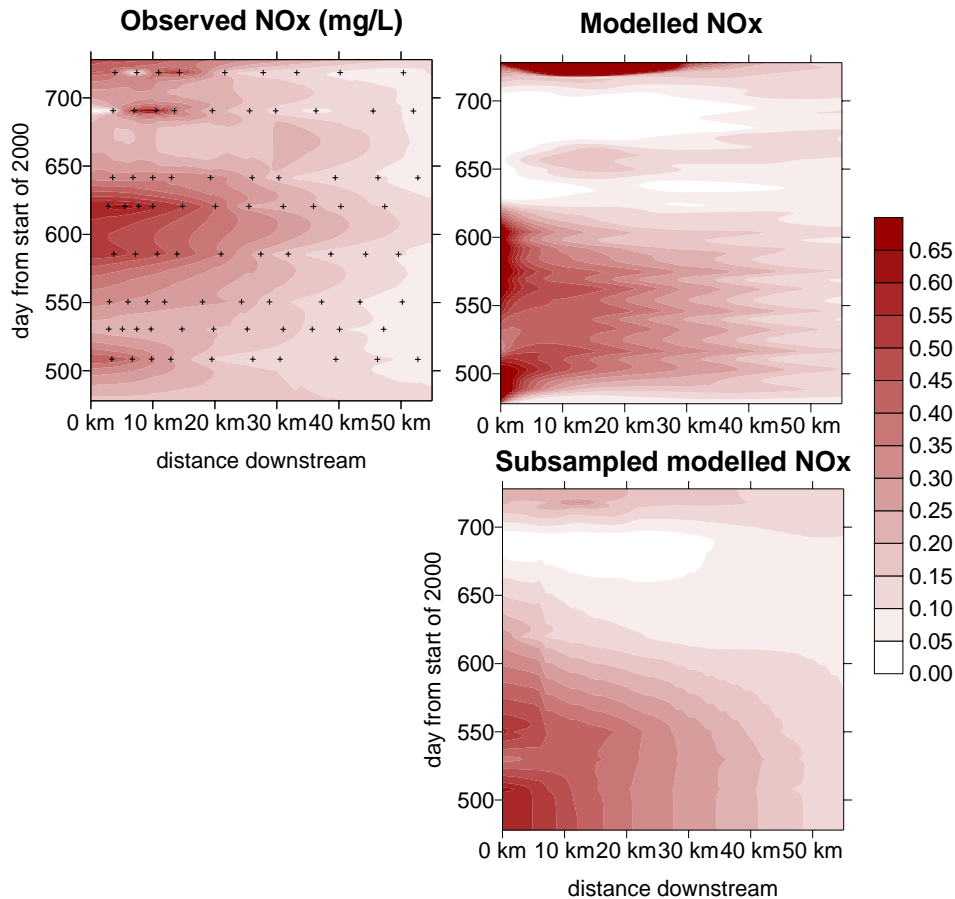


Figure 3.3.1 Observed (left) and simulated (right) NOx. Sampling points are shown as crosses. Top right: daily model output. Bottom right: model output subsampled at the times of field observations and interpolated between sampling dates. The y-axis shows the time, measured in days since 1 January 2000. The contours cover the low-flow period used for modelling.

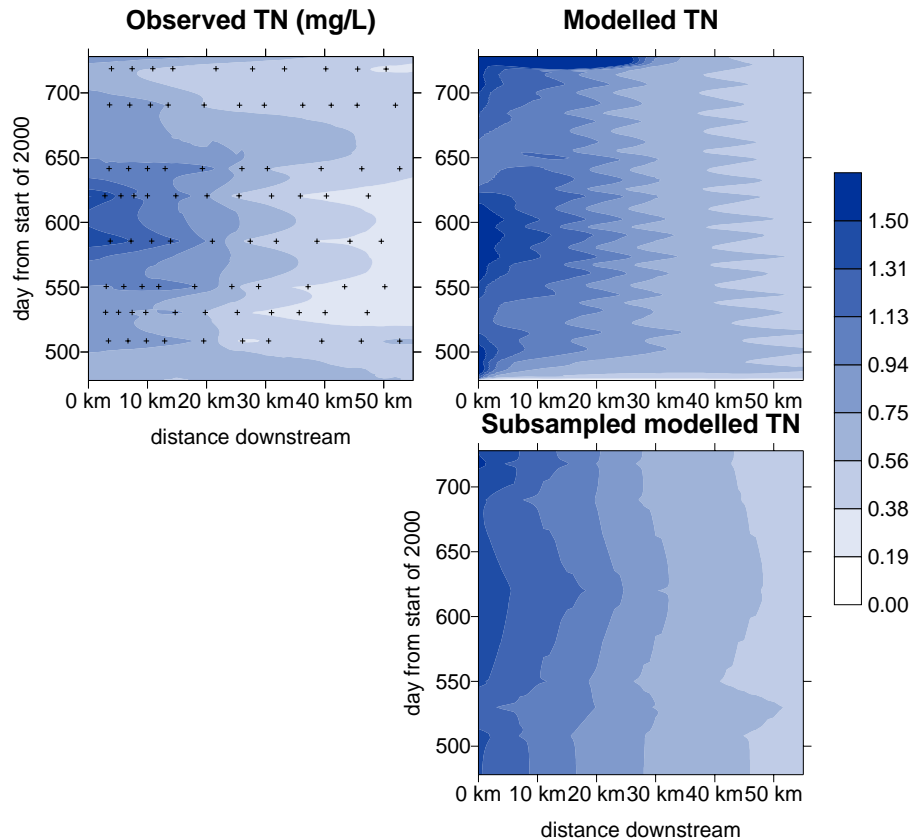


Figure 3.3.2 Observed (left) and simulated (right) total nitrogen. Sampling points are shown as crosses. Top right: daily model output. Bottom right: model output subsampled at the times of field observations and interpolated between sampling dates.

Simulated TSS concentrations at the landward end of the estuary are not as temporally variable as observed TSS concentrations, perhaps as a result of the limited temporal resolution of data for TSS concentrations at the up-estuary boundary. As a result, light conditions in the model are too consistent at the landward end of the estuary. In the field, chlorophyll *a* concentrations are strongly correlated with estimated Secchi depths (Webster et al. 2003) and phytoplankton growth appears to be light-limited. Phytoplankton production occurs primarily in the landward half of the estuary and the budgets suggest that chlorophyll *a* further down estuary has mostly been advected from further up the estuary. Hence, it is not possible to get reasonable simulations of phytoplankton production or chlorophyll *a* concentrations without obtaining adequate model representation of the up-estuary underwater light climate.

For the pilot model, therefore, we set an incident daily light dose that varied according to the water-column light dose calculated from measured incident light and measured light attenuation at a point 10 km downstream from the Barrage. This provided a temporally variable light field to drive primary production in the simulated estuary. Because measurements were available on only a monthly basis and because the light dose calculated by this method is based on attenuation coefficients at a single point, this approach cannot capture the true variability of light within the estuary. Further, because it relies on measured attenuation coefficients, it would be difficult to apply in a predictive sense to scenario simulations. As development of the model continues in the next stage of the project, it is therefore important to ensure that light attenuation in the most productive, landward half of the estuary is accurately simulated.

Nonetheless, the pilot model, with inputs as described, is able to reproduce to a reasonable degree observed chlorophyll *a* concentrations, due primarily to diatoms (Fig. 3.3.3). The model suggests that the upper estuary is very productive, with gross primary production approximately 21 times net production. To calibrate the model, it was necessary to assume a relatively low maximum growth rate at 15°C for large phytoplankton (0.55 d^{-1}) and strong removal processes, with large phytoplankton settling at approximately 4 m d^{-1} , decaying in sediments at a rate of 0.25 d^{-1} and being grazed in the water column by large zooplankton entering the system at 0.08 mg N L^{-1} . In reality, it is likely that a more complex array of factors, including grazing by benthic invertebrates and jellyfish, is responsible for the high rate of removal of phytoplankton from the upper estuary in particular. Dense communities (in places, $>2000 \text{ m}^{-2}$) of a mat-forming mussel, *Amygdalum* cf. *glaberrima*, have been observed in the upper estuary (Currie and Small 2002) and these are likely to contribute to strong grazing pressure. These factors may be explored in more detail as the model is further developed.

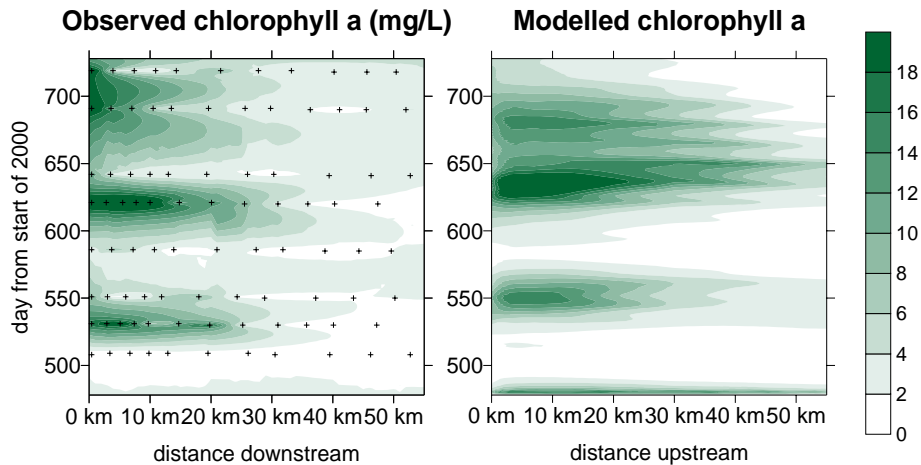


Figure 3.3.3 Observed (left) and simulated (right) chlorophyll a in Fitzroy Estuary during the low flow period. Sampling points are shown as crosses.

As well as phytoplankton, benthic microalgae (Fig. 3.3.4) and benthic macrophytes (Fig. 3.3.5) contribute to primary production in the model. In this simulation, microphytobenthos production occurred primarily in the upper estuary, as for phytoplankton. Modelled growth of microphytobenthos (MPB) in the lower reaches depends on the area and gradient of intertidal mudflats. These factors were not well defined in this pilot model, but a “best guess” morphometry was specified on the basis of the available bathymetric data for the estuary. Initial results suggest that production due to microphytobenthos in the estuary may amount to only 1.5% of total gross primary production, with the majority due to rapidly recycled phytoplankton production, however there is at this stage little quantitative information about microphytobenthos in the estuary to properly calibrate this part of the model. This should be remedied in the next stage of the project and this estimate may very well change substantially as the model is refined.

Growth of benthic macrophytes is restricted to areas in which the water is relatively shallow or clear (Fig. 3.3.5). As for microphytobenthos, macrophytes in the model appear to contribute relatively little to the total primary production of the estuary.

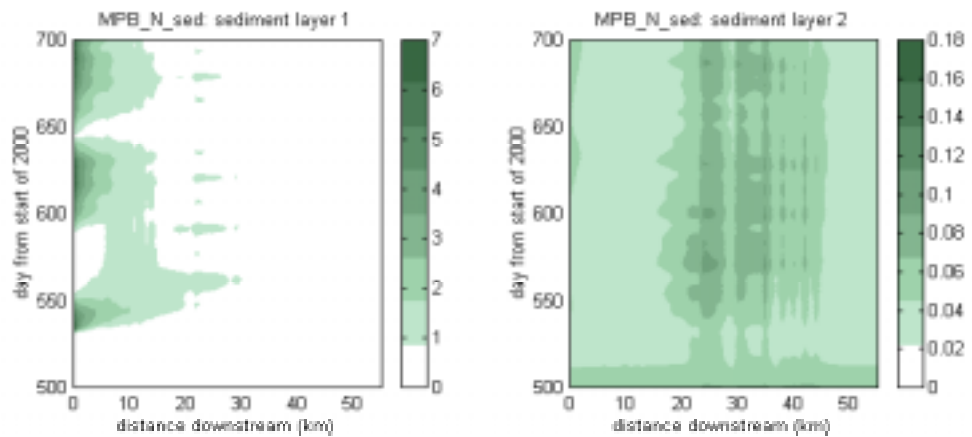


Figure 3.3.4 Simulated concentrations of microphytobenthos concentrations (mg N m^{-3}) in the surface (left) and bottom (right) sediment layers. The surface sediment layer is approximately 5 mm thick, the underlying layer has a variable thickness.

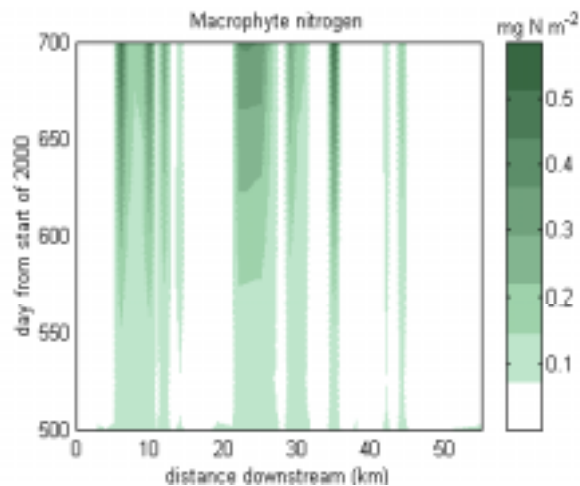


Figure 3.3.5 Simulated concentration of benthic macrophytes.

4 Conclusions

A coupled 1-D hydrodynamic-sediment transport model has been developed and applied to the Fitzroy Estuary. These models were used to support a biogeochemical model for simulating the fate of nutrients and primary production within the estuary. The hydrodynamic module has been calibrated against surface elevation data at Lakes Creek (a site located towards the head of the estuary) and against the whole-estuary data for salinity. The sediment transport module has been calibrated against suspended sediment concentrations measured during a monthly monitoring program of one-year duration.

The calibrated model predicts asymmetric tidal currents and a subsequent upstream pumping of sediments into estuary. Episodic river flows produce short-term flushing of sediments out of the estuary. However under low-flow conditions and over the annual time scale (for the period modelled), the net balance between river loads, sediment discharge to ocean, and up-estuary pumping is an accumulation of sediment in the estuary.

The biogeochemical model successfully reproduces the range and many aspects of the overall patterns observed in nitrogen and chlorophyll *a* concentrations in the estuary, when forced with estimated loadings from the sewage treatment plant and meatworks, plus temporally varying incident light. The model shows that the upper estuary is the most productive area of the model domain, with gross primary production exceeding net production by many times. Phytoplankton in the lower estuary appears to be mostly due to downstream advection.

An idealised scenario has been used to evaluate the likely impact of an elevated river discharge on the sediment fluxes. The model has been run using the same settings as used for calibration study, but river flow increased three times. According to the scenario simulations, increasing peak flows from 660 to 2000 m³s⁻¹ reduces the annual accumulation of river sediments in the estuary from ~ 90 to 35% of total input, and reduces the net input of sediments from Keppel Bay by approximately three times. Given the constraints in the 1-D model formulation and uncertainties in the boundary conditions, these numerical estimates should be considered as indicative rather than definitive.

The Fitzroy Estuary and Keppel Bay are closely interactive estuarine and coastal zones. Consequently, the estuary is sensitive to hydrodynamic and transport conditions in the outside coastal waters. Further progress in understanding estuarine fluxes and evaluating their potential impact on the coastal ocean could be based on numerical modelling for a coupled Fitzroy Estuary and Keppel Bay system using a two- or three-dimensional model, which would allow for the resolution of sediment concentration variation in the water column.

Priorities for further development of the biogeochemical model include improving prediction of light attenuation, verification and calibration of microphytobenthos production and biomass, and application of the model to high-flow periods. These developments will lead to an improved estimate of productivity in the intertidal zone, which at present represents an important gap in our understanding of Fitzroy Estuary and other tropic macrotidal estuaries in Australia. Further work on modelling of intertidal productivity will complement field and laboratory studies being conducted as part of the Fitzroy Contaminants (AC) subproject.

Another priority for modelling in the next stage of the CRC is to look more closely at denitrification in the estuary and its mudflats. Denitrification has been found to be a major nitrogen sink in several Australian estuaries (Harris et al. 1996), while in other estuaries it may be less important (Fredericks et al. 2002). Accurate modelling of denitrification will deliver an improved understanding of nitrogen cycling and removal within the system. Again, this will be complemented by field and laboratory studies.

5 References

- Annual water statistics 2001-2002 Dep of Natural Resources and Mines Report.
- Ariathurai R., Krone R. B. (1976.) Finite element model for cohesive sediment transport. *J. Hydraul. Div. ASCE*, 104, HY2, 323-328.
- Baird, M.E. and S.M. Emsley 1999. Towards a mechanistic model of plankton population dynamics. *Journal of Plankton Research* 21: 85-126.
- Connell D. W., Bycroft B. M. Miller G. J. & Lather P. (1981). Effects of a barrage on flushing and water quality in the Fitzroy River estuary, Queensland. *Australian Journal of Marine and Freshwater Research*, 32:57-63.
- Currie, D. R. and Small, K. J. 2002. Macrobenthic Community Structure in the Fitzroy River Estuary, Queensland. CRC for Coastal Zone Estuary and Waterway Management.
- Ford, P.W., Douglas, G., Hargreaves, P., Lemckert, C., Moss, A., Noble, R., Packett, R., Reville, A., Robson, B., Tillman, P., Webster, I.T. (2003) Carbon and Nutrient Cycling in Subtropical Estuaries, Final Report to CRC Coastal Zone, Estuary, and Waterway Management for project FH-1.
- Fredericks, D. J., Palmer, D. W., Smith, C. S., and Heggie, D. T. 2002. Benthic Fluxes and Nutrient Recycling in the Swan Estuary. Canberra, Australia, Geoscience Australia.
- Goto, N., Mitamura, O., and Terai, H. 2000. Seasonal variation in primary production of microphytobenthos at the Isshiki intertidal flat in Mikawa Bay. *Limnology* 1(2), 0133-0138.
- Harris, G. P., Batley, G., Fox, D., Hall, D., Jernakoff, P., Molloy, R., Murray, A., Newell, B., Parslow, J., Skyring, G., and Walker, S. 1996. Port Phillip Bay Environmental Study: Final Report. Dickson, ACT, Australia, CSIRO.
- Herzfeld M, Waring J., Parslow J., Margvelashvili N., Sakov P. and Andrewartha J. (2002.) MECO: Model for Estuaries and Coastal Oceans, scientific manual. CSIRO Marine Research.
- Howes T., Lemckert C., and Moss A. The Use of Long Term Deployments for Estuarine Water Quality Monitoring: Brisbane River Turbidity. Coastal CRC publication, Ref ID ANZQL0131000393.
- MacIntyre, H. L. and Cullen, J. J. 1996. Fine-scale vertical resolution of chlorophyll and photosynthetic parameters in shallow-water benthos. *Oceanographic Literature Review* 43(2), 133.

- Margvelashvili N., Andrewartha J., Herzfeld M, Parslow J., Sakov P. Waring J. (2002). "MECOSED – Model for Estuarine and Coastal Sediment Transport, Scientific Manual". CSIRO Marine Research.
- Murray, A.G. and Parslow, J.S. 1999a. The analysis of alternative formulations in a simple model of a coastal ecosystem. *Ecological Modelling* 119: 149-166.
- Murray, A.G. and Parslow, J.S. 1999b. Modelling of nutrient impacts in Port Phillip Bay - a semi-enclosed marine Australian ecosystem. *Marine and Freshwater Research* 50: 597-611.
- Murray, A.G. and Parslow, J.S. 1997. Port Phillip Bay Integrated Model: Final Report. Canberra, CSIRO Division of Marine Research.
- Reed C.W, Neidoroda A.W., Swift D.J.P. 1999. Modelling sediment entrainment and transport processes limited by bed armoring. *Marine Geology* 154(1999), pp : 143-154.
- Rochford D.J. (1951.) Studies in Australian estuarine hydrology.I.Introductory and comparative features. *Asust.J.Mar.Freshwater. Res.* 2, 1-116
- Smith J.D., McLean S.R. Spatially averaged flow over a wavy bed. *J. Geophys. Res.*, 82, 1977, 1735-1746.Taylor B., Jones M. (2000.) National Land and Water Resources Audit. Fitzroy Audit Summary Report 2000, 21 p.
- Soeteart, K., Middelburg, J.L. , Herman, P.M.J. and Buis, K. 2000. On the coupling of benthic and pelagic biogeochemical models. *Earth Sciences Reviews* 51: 173-201.
- Teeter A., Johnson B., Berger C., Stelling G., Scheffner N., Garcia M., Parchure T. (2001.) Hydrodynamic and sediment transport modelling with emphasis on shallow water, vegetated areas (lakes, reservoirs, estuaries and lagoons). *Hydrobiologia* 444:, 1-23.
- Walker, S.J. 1999 Coupled hydrodynamic and transport models of Port Phillip Bay, a semi-enclosed bay in south-eastern Australia. *Marine and Freshwater research.* 50:, 469-481.
- Webster, I.T., Ford, P.W., Robson, B., Margvelashvili, N., and Parslow, J.S. 2003 Conceptual Models of the Hydrodynamics, Fine-Sediment Dynamics, Biogeochemistry, and Primary Production in the Fitzroy Estuary. Final Report to CRC Coastal Zone, Estuary, and Waterway Management for project CM-2.

Appendix 1. Parameter values used in the sediment and biogeochemical model.

Table A.1 Basic parameters for the sediment model.

Parameter	Description	Model value
$\epsilon_{i,w/b}$	Void ratio of fresh deposits	1.2
τ_e	Critical shear stresses of cohesive sediment erosion (sediments are eroded when bottom shear stress exceeds critical shear stress)	0.3 Nm ⁻²
z_o	Bottom roughness parameter	0.004 m
α	Relaxation rate constant for TSS concentration at the estuarine mouth	0.1 d ⁻¹
h_a	Thickness of the top sediment layer	0.005 m
K_z	Diffusion coefficient for mixing of the solid particles in sediments	10 ⁻⁹ m ² s ⁻¹

Table A.1 Basic parameters for the sediment model.

Parameter	Description	Model value
ZL_E	(Growth efficiency, large zooplankton)	0.38
ZS_E	(Growth efficiency, small zooplankton)	0.38
PhyL_mL	(Natural (linear) mortality rate, large phytoplankton (in sediment))	0.25 d ⁻¹
PhyS_mL	(Natural (linear) mortality rate, small phytoplankton (in sediment))	0.14 d ⁻¹
MA_mL	(Natural (linear) mortality rate, macroalgae)	0.01 d ⁻¹
MPB_mQ	(Natural (quadratic) mortality rate, microphytobenthos)	0.0003 d ⁻¹ (mg N m ⁻³) ⁻¹
ZL_mQ	(Natural (quadratic) mortality rate, large zooplankton)	0.0004 d ⁻¹ (mg N m ⁻³) ⁻¹
ZS_mQ	(Natural (quadratic) mortality rate, small zooplankton)	0.02 d ⁻¹ (mg N m ⁻³) ⁻¹
ZL_FDG	(Fraction of growth inefficiency lost to detritus, large zooplankton)	0.25
ZL_FDM	(Fraction of mortality lost to detritus, large zooplankton)	0.25
ZS_FDG	(Fraction of growth inefficiency lost to detritus, small zooplankton)	0.25
ZS_FDM	(Fraction of mortality lost to detritus, small zooplankton)	0.25
F_LD_RD	(Fraction of labile detritus converted to refractory detritus)	0.3
F_LD_DOM	(Fraction of labile detritus converted to dissolved organic matter)	0.15
NtoCHL	(Nitrogen:Chlorophyll A ratio in phytoplankton by weight)	7.5
k_w	(Background light attenuation coefficient)	0.1 m ⁻¹
k_DOR_N	(DOR_N-specific light attenuation coefficient)	0.0009 m ⁻¹ (mg N m ⁻³) ⁻¹
k_DetL	(Detrital N-specific light attenuation coefficient)	0.0038 m ⁻¹ (mg N m ⁻³) ⁻¹
k_TSS	(TSS-specific light attenuation coefficient)	20.0 m ⁻¹ (kg m ⁻³) ⁻¹
k_C_fw	(CDOM attenuation coefficient of freshwater)	0.1 m ⁻¹
Q10	(Temperature coefficient for rate parameters)	2.0
PLumax	(Maximum growth rate of PL at Tref)	0.55 d ⁻¹
MAumax	(Maximum growth rate of macroalgae at Tref)	0.02 d ⁻¹

FITZROY NUMERICAL MODELS

MAaa	(Nitrogen-specific absorption cross-section of macroalgae)	0.001 m ² mg N ⁻¹
PLrad	(Radius of the large phytoplankton cells)	10e-06 m
PLabsorb	(Absorption coefficient of a PL cell)	50000 m ⁻¹
PLSh	(Sherwood number for the PS dimensionless)	1
PLn	(Number of limiting nutrients)	3
PSumax	(Maximum growth rate of PS at Tref)	1.2 d ⁻¹
PSrad	(Radius of the small phytoplankton cells)	2.5e-06 m
PSabsorb	(Absorption coefficient of a PS cell)	50000 m ⁻¹
PSSh	(Sherwood number for the PL dimensionless)	1
MBumax	(Maximum growth rate of MB at Tref)	0.45 d ⁻¹
MBrad	(Radius of the MB cells)	1.0e-05 m
MBabsorb	(Absorption coefficient of a MB cell)	50000 m ⁻¹
MBSH	(Sherwood number for the PL dimensionless)	1
ZSumax	(Maximum growth rate of ZS at Tref)	3 d ⁻¹
ZSrad	(Radius of the small zooplankton cells)	12.5e-06 m ⁻¹
ZSswim	(Swimming velocity for small zooplankton)	1.0e-4 m s ⁻¹
ZLumax	(Maximum growth rate of ZL at Tref)	0.1 d ⁻¹
ZLrad	(Radius of the large zooplankton cells)	5.0e-04 m ⁻¹
ZLswim	(Swimming velocity for large zooplankton)	2.0e-4 m s ⁻¹
TKEeps	(TKE dissipation in water column)	1.0e-6 m ² s ⁻³
cf	(drag coefficient of the benthic surface)	0.005
Ub	(velocity at the top of the ben. bound. layer)	0.1 m s ⁻¹
ks	(sand-grain roughness of the benthos)	0.1 m
F_RD_DOM	(fraction of refractory detritus that breaks down to DOM)	0.25
r_floc	(rate at which TSS floculates above 10 PSU)	0.01 d ⁻¹
r_DetPL	(Breakdown rate of labile detritus at 106:16:1)	0.1 d ⁻¹
r_DetBL	(Breakdown rate of labile detritus at 550:30:1)	0.1 d ⁻¹
r_RD	(Breakdown rate of refractory detritus)	0.002 d ⁻¹
r_DOM	(Breakdown rate of dissolved organic matter)	0.001 d ⁻¹
Tref	(Reference temperature)	15.0 °C
Plank_resp	(Respiration as a fraction of umax)	0.025
Benth_resp	(Respiration as a fraction of umax)	0.025
KO_aer	(Oxygen half-saturation for aerobic respiration)	500 mg O m ⁻³
r_nit_wc	(Maximal nitrification rate in water column)	0.45 d ⁻¹
r_nit_sed	(Maximal nitrification rate in water sediment)	0.45 d ⁻¹
KO_nit	(Oxygen half-saturation for nitrification)	8000 mg O m ⁻³
Pads_r	(Rate at which P reaches adsorbed/desorbed equilibrium)	1.0 d ⁻¹
r_den	(Maximum denitrification rate)	5.0 d ⁻¹
KO_den	(Oxygen content at 50% denitrification rate)	500.0 mg O m ⁻³
r_floc_sed	(Rate of the TSS floculation in sediment)	0.001 d ⁻¹
r_bury_TSS	(Rate of the TSS burying)	0.001 d ⁻¹